Supplemental Data

Supplemental Methods

Colony-forming unit assay for megakaryocytes (MKs)

The collagen-based MegaCult-C Kit (STEMCELL Technologies) was used for the CFU-MK colony-forming assays. Suspended iPSCs or CB $CD34^+$ cells (7500–10,000 cells) at day 14 in culture were seeded onto one double chamber slide with semiliquid culture medium. After 10~12 days in culture, the CFU-MK colonies were stained with anti-CD41 antibody and counted according to the MegaCult-C protocol (STEMCELL Technologies) under a light microscope (NIKON).

Real-time PCR

The quantitative polymerase chain reaction (qPCR) following reverse transcription (RT-qPCR) or ChIP (ChIP-qPCR) was carried out as previously described.[1] Primers are provided in Table S1.

Table S1. A list of primers used for PCR.

RT-qPCR primers		
Gene ID	Forward primer	Reverse primer
NOTCH1	CGGGTCCACCAGTTTGAATG	GTTGTATTGGTTCGGCACCAT
NOTCH2	TTTGGCAACTAACGTAGAAACTCAAC	TGCCAAGAGCATGAATACAGAGA
NOTCH3	TGATCGGCTCGGTAGTAATGC	GACAACGCTCCCAGGTAGTCA
NOTCH4	CCTCCTAGGGGCTGTTCGAA	GTAGGTGTCCAGCCCATCCT
HES1	GCTGGAGAAGGCGGACATTC	GCACCTCGGTATTAACGCCC
HEY1	AGAGTGCGGACGAGAATGGA	AGCTTAGCAGATCCCTGCTTCT
RUNX1	GCCCCGAGAACCTCGAA	CCGGGCTTGGTCTGATCAT
FLI1	CCAACGAGAGGAGAGTCATCGT	TGCCTCACATGCTCCTGTGT
GATA1	GCCTACAGACACTCCCCAGTCT	CTGGGATCCCCTCCATACAGT
SPI1	CGCCAAACGCACGAGTATT	TCCCAGTAATGGTCGCTATGG
KLF1	GCCTGTTTGGTGGTCTCTTCA	GGTCCATTCGTGGGAAAACC
CEBPA	GAGGGACCGGAGTTATGACAAG	GGCACAGAGGCCAGATACAAG
NOTCH4 intron 29	CAGGGACATGGTGTACCCCTAT	CACCACAAACCCAGCACTGA
Primers for genotype		
Gene ID	Forward primer	Reverse primer
NOTCH1-KO	AAAAGTTTCTACCTGGGGCCA	TTCCTGAGTGGAGAGCCGAG
NOTCH2-KO	GGGATGGTGTCAGGTAGGGA	AAGCACATAACCACCCCTCG
NOTCH3-KO	GTACCAAGCTGAGGACTCCC	AGTCTGGAGGGGAGGTAGTC
NOTCH4-KO	GAAGGAGCCCAGGGTGTTATG	GCTAGAAACGGCTCCCTCTG
NOTCH4 intron 29	CTACTTCCACCGCTCCTTCC	CTGGGGTAACAACCTCCCAC
ChIP-qPCR primers		
Gene ID	Forward primer	Reverse primer
RUNX1 +23kb	CCTGTGGTTTTCTCGCTCTC	ATGCTGACAGCCTCAGATGG
RUNX1 +31kb	AAAGCCACAAAAAGAGATCTGG	AGCACCTGCCAGAAGACATC
NOTCH4 intron 29	GGGTAACAACCTCCCACGTC	TCCTGGGCATCTTTATCGGC

Table S2. A list of guide RNA (gRNA)-targeted DNA sequences.

Gene target	gRNA1	gRNA2
NOTCH1	TGACGTCGATCTCGCATCGG	
NOTCH2	CTCCACCTGCATCGACCGTG	
NOTCH3	CCGCAGCTGCCGAAGCGACG	GGGCACCTGTACCGACCACG
NOTCH4	CAGAGCTGGGCGTTCTGGCA	
NOTCH4 intron 29	GCCTTCACTTGCGCGACCAC	ACAGTCAGGCGCACGAGAGA

Table S3. A list of genes that contain RUNX1-binding sites and are differentially expressed in isogenic *RUNX1*-corrected or mutated (FPD) iPSC-derived CD34$^+$ cells.

Genes	Fold Change	P-value	FDR	Entrez Gene Name
PPP2R2C	12.03	3.85E-06	1.49E-03	Protein phosphatase 2 regulatory subunit B gamma
C15orf53	8.59	5.67E-05	1.29E-02	Chromosome 15 Open Reading Frame 53
BCAN	8.14	1.14E-06	6.68E-04	Brevican
LGALSL	7.76	2.93E-10	8.58E-07	Galectin Like
VWA3B	6.49	8.77E-05	1.78E-02	Von Willebrand Factor A Domain Containing 3B
TTC39B	5.83	2.69E-06	1.10E-03	Tetratricopeptide Repeat Domain 39B
SEC14L5	5.31	3.06E-04	4.14E-02	SEC14 Like Lipid Binding 5
EPB49	5.21	2.29E-05	6.16E-03	Dematin Actin Binding Protein
MPZL3	4.71	2.34E-04	3.52E-02	Myelin Protein Zero Like 3
ITGB3	4.45	1.28E-04	2.25E-02	Integrin Subunit Beta 3; CD61; GPIIIa
PF4	4.23	3.75E-11	1.30E-07	platelet factor 4
C11orf21	4.21	1.65E-05	4.98E-03	Chromosome 11 Open Reading Frame 21
RSPH1	4.18	1.00E-04	1.96E-02	Radial Spoke Head 1 Homolog
RGS9	4.14	1.28E-04	2.25E-02	Regulator Of G Protein Signaling 9
FHOD3	4.11	7.52E-06	2.57E-03	Formin Homology 2 Domain Containing 3
RTN1	4.04	1.27E-06	6.97E-04	Reticulon 1
DAAM1	3.96	2.66E-07	2.10E-04	Dishevelled Associated Activator Of Morphogenesis 1
CD226	3.94	9.32E-05	1.85E-02	CD226 Molecule
GCSAML	3.88	3.40E-04	4.43E-02	Germinal Center Associated Signaling And Motility Like
MYLK	3.66	3.03E-04	4.14E-02	Myosin Light Chain Kinase
ADCY6	3.66	1.68E-06	7.48E-04	Adenylate Cyclase 6
THBS1	3.40	1.45E-06	7.23E-04	Thrombospondin 1
MFSD6	3.33	4.74E-06	1.70E-03	Major Facilitator Superfamily Domain Containing 6
LOC100505702	3.20	3.46E-04	4.48E-02	
LDLRAD4	3.04	2.91E-05	7.54E-03	Low Density Lipoprotein Receptor Class A Domain Containing 4
ZNF175	2.97	1.34E-04	2.30E-02	Zinc Finger Protein 175
MFSD2B	2.82	3.63E-04	4.65E-02	Major Facilitator Superfamily Domain Containing 2B
PIK3CB	2.78	4.44E-05	1.07E-02	Phosphatidylinositol-4,5-Bisphosphate 3-Kinase Catalytic Subunit Beta
COL24A1	2.72	1.96E-05	5.43E-03	Collagen Type XXIV Alpha 1 Chain
ST8SIA6	2.70	7.04E-05	1.50E-02	ST8 Alpha-N-Acetyl-Neuraminide Alpha-2,8-Sialyltransferase 6
SLC37A1	2.63	8.45E-06	2.84E-03	Solute Carrier Family 37 Member 1
SAMD14	2.62	5.61E-05	1.29E-02	Sterile Alpha Motif Domain Containing 14
ARHGAP6	2.51	1.51E-04	2.48E-02	Rho GTPase Activating Protein 6
ABCC4	2.51	1.53E-04	2.48E-02	ATP Binding Cassette Subfamily C Member 4
UBASH3B	2.44	4.16E-05	1.03E-02	Ubiquitin Associated And SH3 Domain Containing B
CD47	2.26	1.40E-04	2.36E-02	CD47 Molecule
F2R	2.19	2.32E-04	3.52E-02	Coagulation Factor II Thrombin Receptor
CD44	-2.34	3.78E-04	4.76E-02	CD44 Molecule (Indian Blood Group)
PRCP	-2.48	1.06E-04	2.00E-02	Prolylcarboxypeptidase

DUSP1	-2.82	2.16E-05	5.90E-03	Dual Specificity Phosphatase 1
KLF6	-2.92	1.21E-04	2.16E-02	Kruppel Like Factor 6
COLEC12	-2.99	2.45E-04	3.60E-02	Collectin Subfamily Member 12
GAS7	-3.02	2.13E-04	3.25E-02	Growth Arrest Specific 7
TIAM1	-3.29	2.72E-04	3.90E-02	T-Cell Lymphoma Invasion And Metastasis 1
PROCR	-3.52	3.23E-04	4.29E-02	Protein C Receptor
GCNT1	-3.66	2.52E-04	3.67E-02	Glucosaminyl (N-Acetyl) Transferase 1, Core 2
IMPA2	-3.67	3.29E-04	4.34E-02	Inositol Monophosphatase 2
KIAA1462	-3.86	9.19E-07	6.07E-04	Junctional Cadherin 5 Associated
APCDD1	-4.40	3.07E-04	4.14E-02	APC Down-Regulated 1
TNFSF10	-4.46	1.03E-04	1.97E-02	TNF Superfamily Member 10
GALNTL4	-4.48	1.02E-04	1.97E-02	Polypeptide N-Acetylgalactosaminyltransferase 18
FOS	-4.66	3.77E-07	2.76E-04	Fos Proto-Oncogene, AP-1 Transcription Factor Subunit
VEGFC	-4.68	4.04E-04	4.86E-02	Vascular Endothelial Growth Factor C
SHE	-4.74	1.29E-06	6.97E-04	Src Homology 2 Domain Containing E
WFS1	-4.74	3.49E-04	4.49E-02	Wolframin ER Transmembrane Glycoprotein
RPS6KA2	-4.87	2.16E-07	1.84E-04	Ribosomal Protein S6 Kinase A2
ERG	-5.11	6.92E-08	7.09E-05	ERG, ETS Transcription Factor
NOTCH4	-5.52	3.04E-08	3.66E-05	Notch 4
LRIG3	-5.58	1.61E-08	2.20E-05	Leucine Rich Repeats And Immunoglobulin Like Domains 3
BST2	-5.61	4.62E-05	1.10E-02	Bone Marrow Stromal Cell Antigen 2
CHST1	-5.65	3.76E-04	4.76E-02	Carbohydrate Sulfotransferase 1
SORL1	-5.73	2.25E-07	1.84E-04	Sortilin Related Receptor 1
KLF2	-7.33	3.71E-06	1.46E-03	Kruppel Like Factor 2
MADCAM1	-10.80	2.07E-04	3.22E-02	Mucosal Vascular Addressin Cell Adhesion Molecule 1

Figure S1

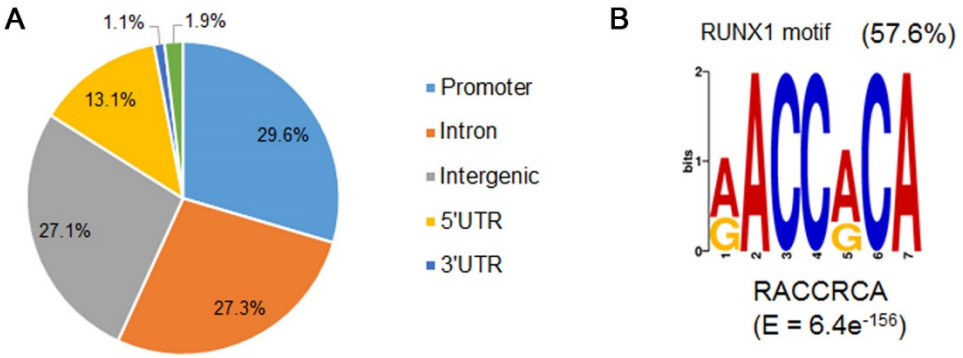

Figure S1. Genome-wide occupancy of RUNX1 in BC1 iPSC-CD34$^+$ cells. (A) Pie chart showing the distribution of RUNX1 binding peaks in BC1 iPSC-CD34$^+$ cells. (B) De novo motif discovery of sequences bound by RUNX1 in BC1 iPSC-CD34$^+$ cells is consistent with the known RUNX1 motif.

Figure S2

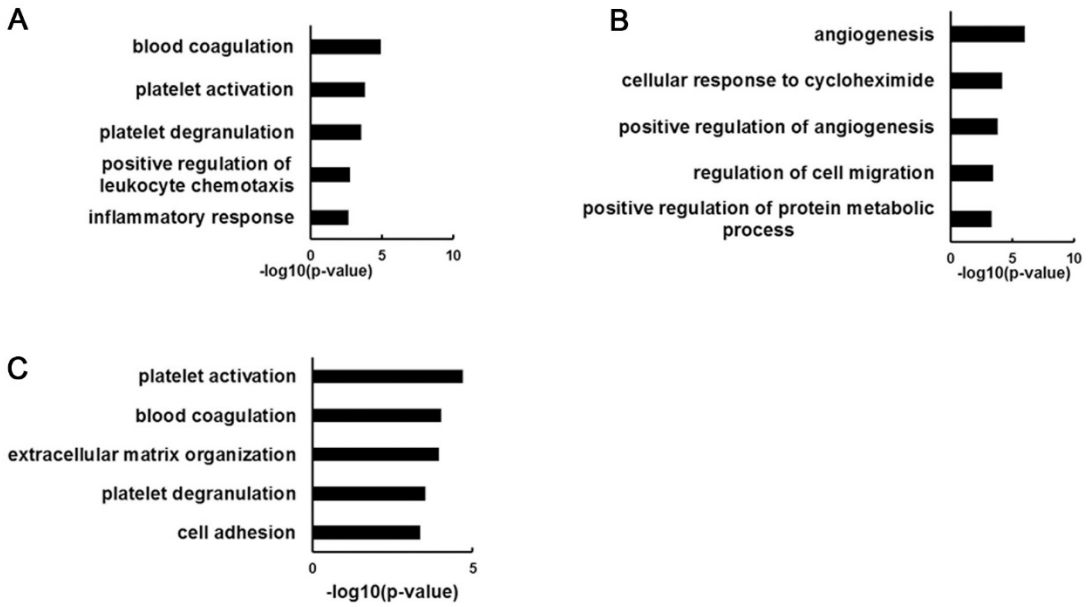

Figure S2. Function enrichment analysis of differential expression genes. (A) Gene Ontology (GO) enrichment analysis of upregulated genes in *RUNX1*-corrected-CD34$^+$ cells. (B) GO enrichment analysis of downregulated genes in *RUNX1*-corrected-CD34$^+$ cells. (C) GO enrichment analysis of RUNX1 binding genes that are upregulated in *RUNX1*-corrected-CD34$^+$ cells.

Figure S3

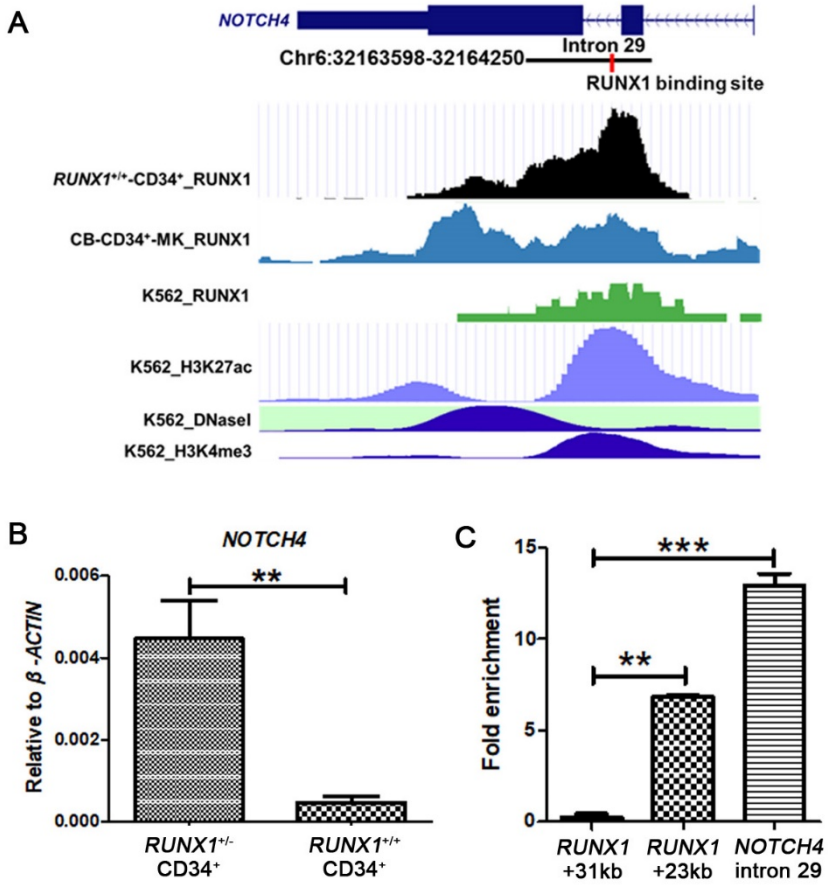

Figure S3. *NOTCH4* is negatively controlled by RUNX1 via a DNA element within the intron 29 locus. (A) RUNX1 binding region in intron 29 of *NOTCH4* is marked in the gene structure as a horizontal black line and the RUNX1 consensus binding site as a vertical red line. DNaseI hypersensitive sites and H3K4me3 and H3K27ac histone modifications in K562 cells are present in the RUNX1 binding region on the UCSC genome browser. Published RUNX1 binding profiles in K562 and CB (cord blood) CD34$^+$ induced megakaryocyte (MK) cells are also presented in the RUNX1 binding region.[2,3] (B) Downregulation of *NOTCH4* detected by RNA-Seq was validated by RT-qPCR using cDNA from *RUNX1*$^{+/-}$ CD34$^+$ and *RUNX1*$^{+/+}$ CD34$^+$ cells. *β -ACTIN* was used as an internal control. Data are shown as the means ± SEM, n = 2 (biological replicates). ***P* < .01. (C) Confirmation of RUNX1 occupancy regions in intron 29 of the *NOTCH4* gene locus by ChIP-qPCR. The *RUNX1* intron 1 +23 kb enhancer was used as a positive region and the *RUNX1* +31 kb as a corresponding negative region.[2] Signals detected by RUNX1 antibody were compared to input. Data are shown as the means ± SEM, n = 3 (technical replicates). ***P* < .01; ****P* < .001.

Figure S4

A

	RUNX1 binding	Fold change
NOTCH1	Yes	1.13 (*p*=0.61, FDR=1)
NOTCH2	Yes	0.82 (*p*=0.5, FDR=1)
NOTCH3	No	0.32 (*p*=0.31, FDR=1)
NOTCH4	Yes	0.18 (*p*=3.0E-08, FDR=3.7E-05)

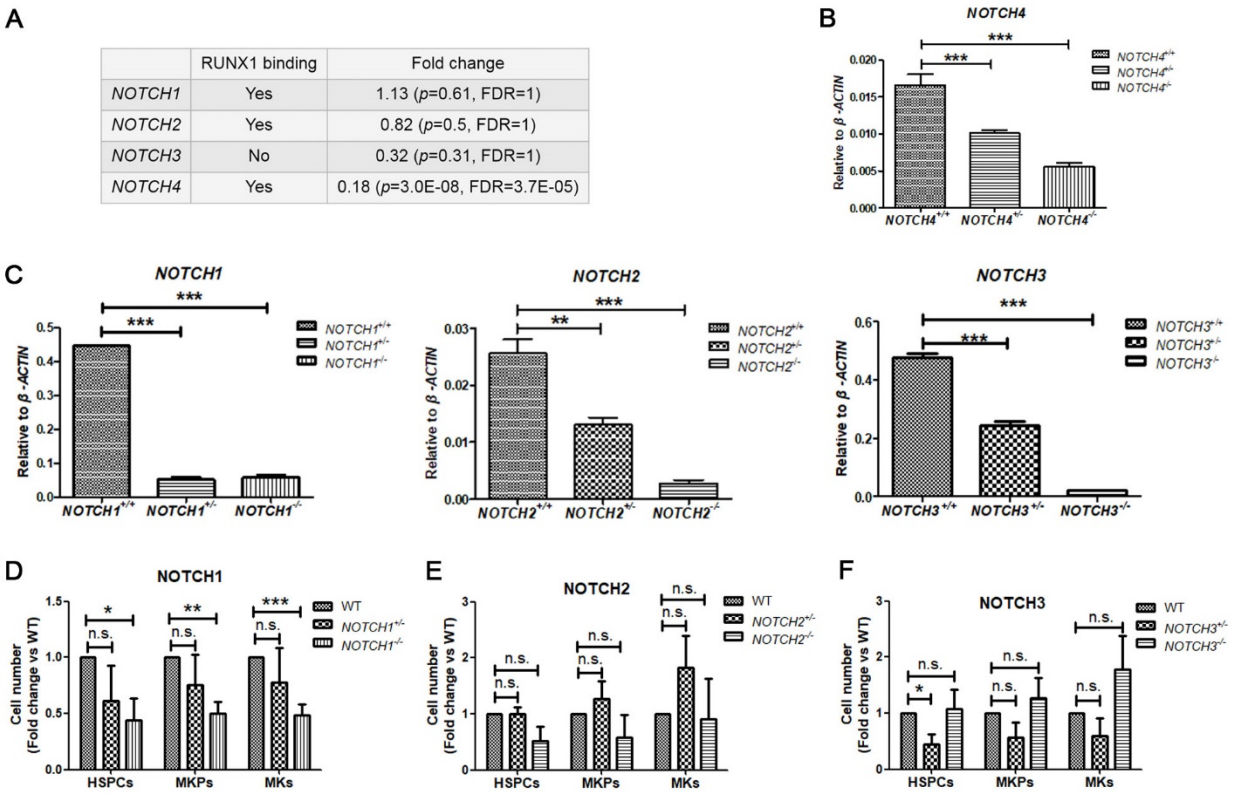

Figure S4. Knockout of *NOTCH1, 2,* and *3* do not promote hematopoiesis or megakaryopoiesis. (A) The list shows whether Notch receptor genes (*NOTCH1-4*) are bound by RUNX1 and the fold change of gene expression in *RUNX1*$^{+/+}$ CD34^{+} cells compared with RUNX1$^{+/-}$ CD34^{+} cells. (B) RT-qPCR analysis of *NOTCH4* mRNA level in each corresponding gene KO iPSCs. *β -ACTIN* was used as an internal control. Data are shown as means ± SEM, n = 3. ****P* < .001. (C) RT-qPCR analysis of *NOTCH1-3* mRNA level in each corresponding gene KO iPSCs. *β -ACTIN* was used as an internal control. Data are shown as means ± SEM, n = 3. ***P* < .01; ****P* < .001. (D) Bar graph depicting fold changes of the cell numbers of hematopoietic stem and progenitor cells (HSPCs), megakaryocyte progenitors (MKPs), and megakaryocytes (MKs) on day 14 in hematopoietic cells derived from *NOTCH1*$^{-/-}$, *NOTCH1*$^{+/-}$, or WT cells. Data are shown as means ± SEM, n = 3. **P* < .05; ***P* < .01; ****P* < .001. n.s., no significant. (E) Bar graph depicting fold changes of the cell numbers of HSPCs, MKPs, and MKs on day 14 in hematopoietic cells derived from *NOTCH2*$^{-/-}$, *NOTCH2*$^{+/-}$, or WT cells. Data are shown as means ± SEM, n = 3. n.s., no significant. (F) Bar graph depicting fold changes of the cell numbers of HSPCs, MKPs, and MKs on day 14 in hematopoietic cells derived from *NOTCH3*$^{-/-}$, *NOTCH3*$^{+/-}$, or WT cells. Data are shown as means ± SEM, n = 3. **P* < .05; n.s., no significant.

Figure S5

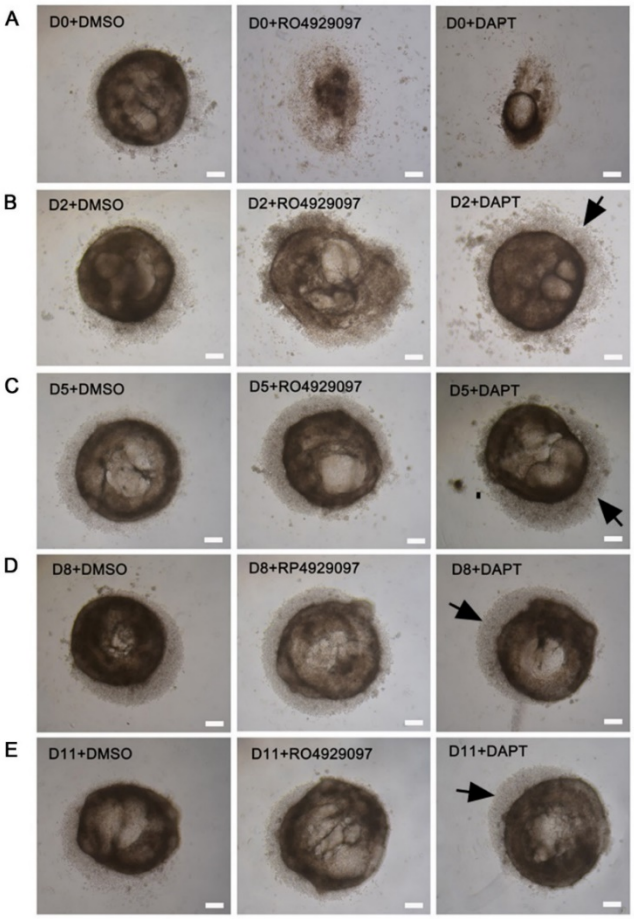

Figure S5. Inhibition of Notch signaling from days 0, 2, 5, 8, or 11 has different effects on megakaryopoiesis. Representative images of day 14 embryoid bodies derived from BC1 iPSCs after addition of 10μM gamma secretase inhibitors (GSIs; RO4929097, DAPT) or DMSO (control) from different time points (day 0 (A), day 2 (B), day 5 (C), day 8 (D), and day 11 (E)). Arrows indicate surrounding cells. Scale bars = 100 μm.

Figure S6

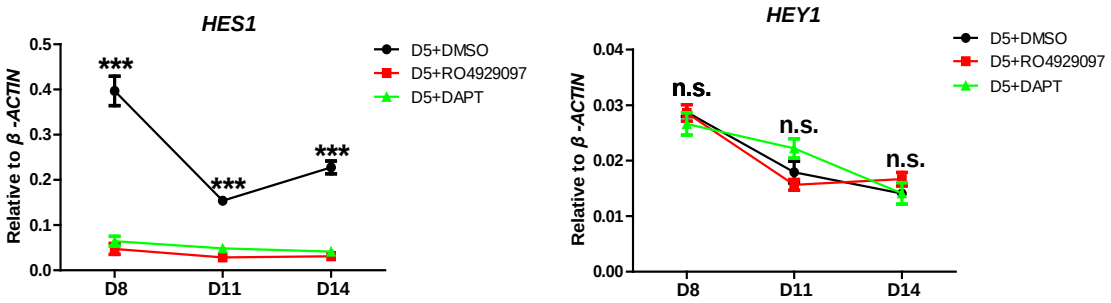

Figure S6. GSI addition results in NOTCH inhibition by suppressing HES1 expression. RT-qPCR analysis of *HES1* and *HEY1* mRNA level at day 8, 11 and 14 after 10μM GSIs (RO4929097/DAPT) or DMSO (control) addition from day 5. *β -ACTIN* was used as an internal control. Data are shown as means ± SEM, n = 3. ***$P < .001$. n.s., no significant.

Figure S7

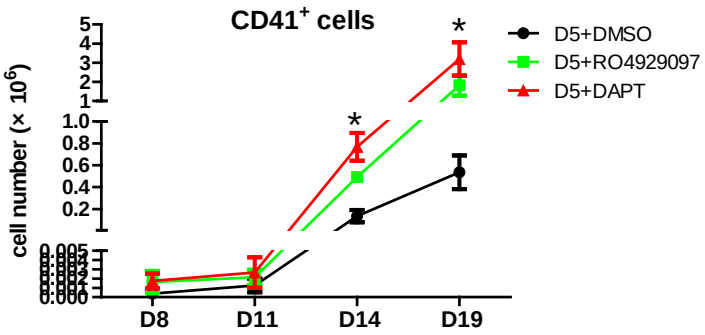

Figure S7. GSIs promote the expansion of CD41⁺ MKs that are generated from BC1 cells. The cell number of megakaryocytes (CD41⁺ cells) at day 8, 11, 14 and 19 after 10μM GSIs (RO4929097/DAPT) or DMSO (control) addition from day 5. Data are shown as means ± SEM, n = 3. **P*< .05.

Figure S8

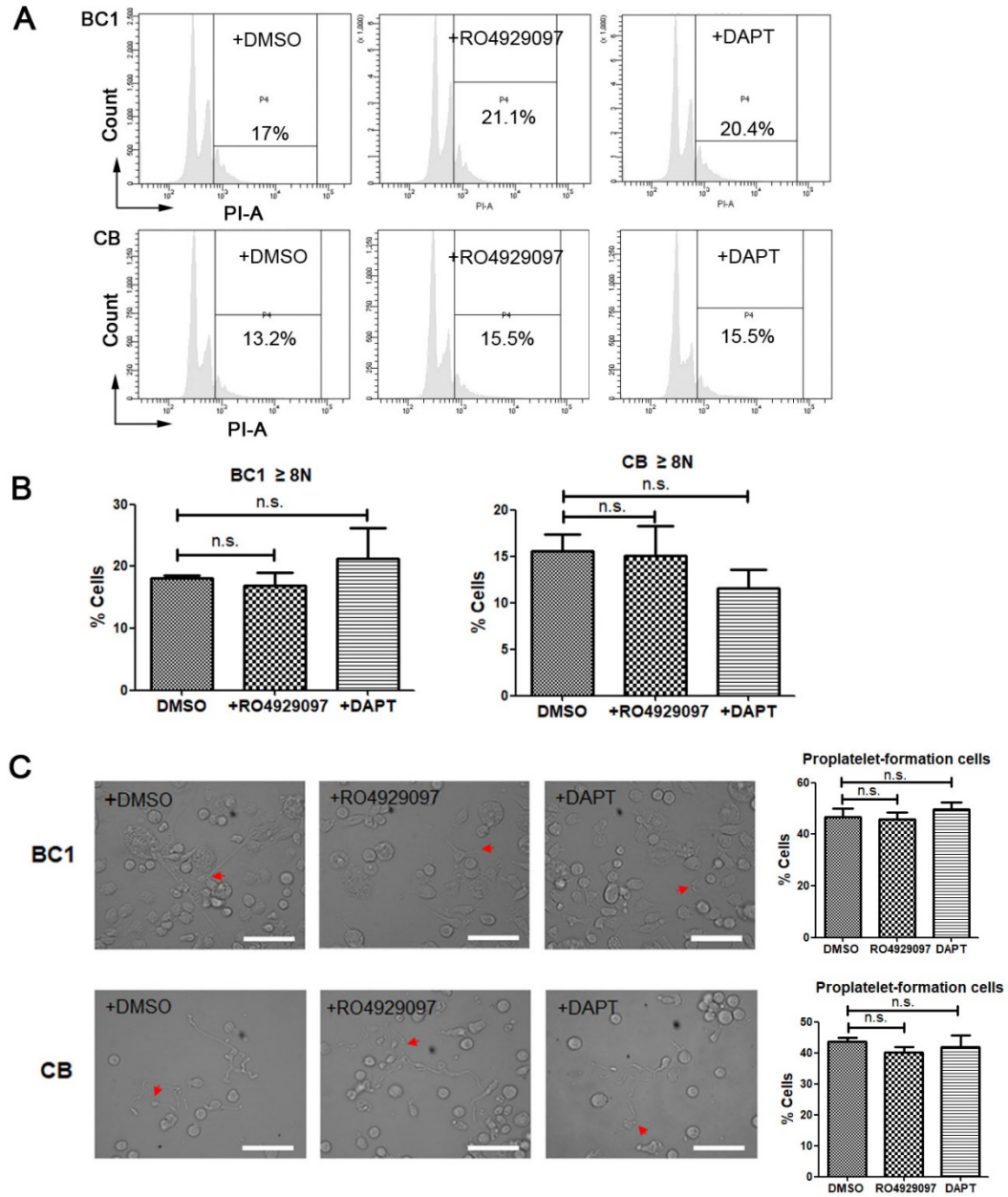

Figure S8. Characterization of MK cells that are generated from human iPS cells (BC1) or cord blood CD34⁺ cells in the presence of GSIs (RO4929097 or DAPT) or DMSO (control). (A) DNA content analysis by flow cytometry of CD61⁺ cells with DNA content ≥ 8N, with addition of 10μM gamma secretase inhibitors (GSIs; RO4929097 or DAPT) or DMSO (control). (B) Bar graph depicting the proportion of CD61⁺ cells with DNA content ≥ 8N. Data are shown as the means ± SEM, n = 3. n.s., no significant. (C) Phase contrast picture of spontaneous proplatelet-forming MKs and the percentage of MKs forming proplatelets, with addition of 10μM gamma secretase inhibitors (GSIs; RO4929097 or DAPT) or DMSO (control). Scale bars = 100 μm. Data are shown as the means ± SEM, n = 3. n.s., no significant.

Figure S9

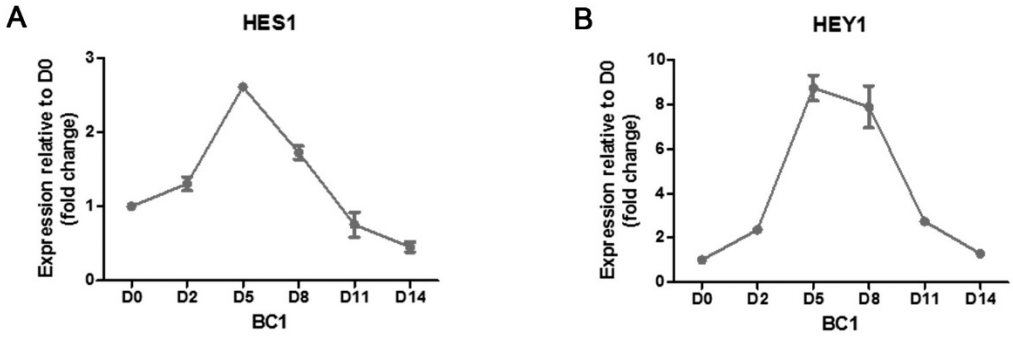

Figure S9. Expression of *HES1* and *HEY1* during differentiation. (A-B) RT-qPCR analysis of *HES1* or *HEY1* mRNA level throughout differentiation of BC1 iPSCs. *β -ACTIN* was used as an internal control. Results from day 0 were set to 1. Data are shown as means ± SEM, n = 3.

Figure S10

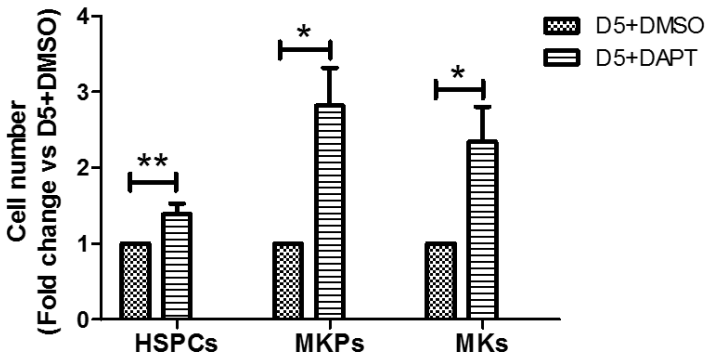

Figure S10. Inhibition of Notch signaling promotes megakaryopoiesis from different iPSCs. Bar graph depicting fold changes of the cell numbers of hematopoietic stem and progenitor cells (HSPCs), megakaryocyte progenitors (MKPs), and megakaryocytes (MKs) on day 14 derived from iPSC-U21 cells, with addition of after 10μM gamma secretase inhibitors (GSIs; DAPT) or DMSO (control) from day 5. Data are shown as means ± SEM, n = 5. **P*< .05; ***P* < .01.

Figure S11

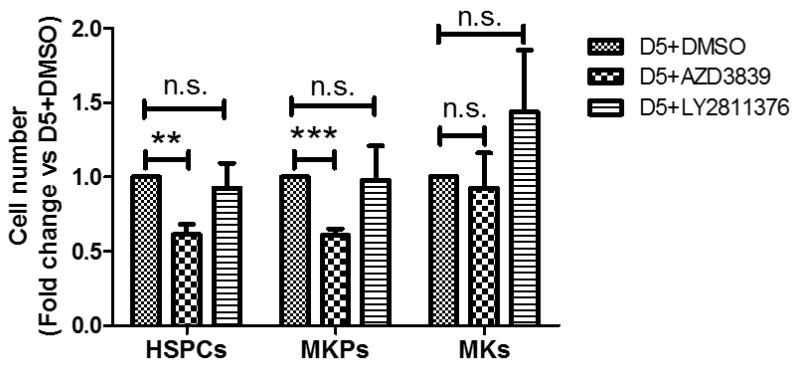

Figure S11. Beta-secretase inhibitors do not promote megakaryopoiesis. Bar graph depicting fold changes of the cell numbers of hematopoietic stem and progenitor cells (HSPCs), megakaryocyte progenitors (MKPs), and megakaryocytes (MKs) on day 14 in hematopoietic cells derived from BC1 iPSCs cells, with addition of after 10μM beta-secretase inhibitors (AZD3839, LY2811376) or DMSO (control) from day 2. Data are shown as the means ± SEM, n = 3. n.s., no significant.

Figure S12

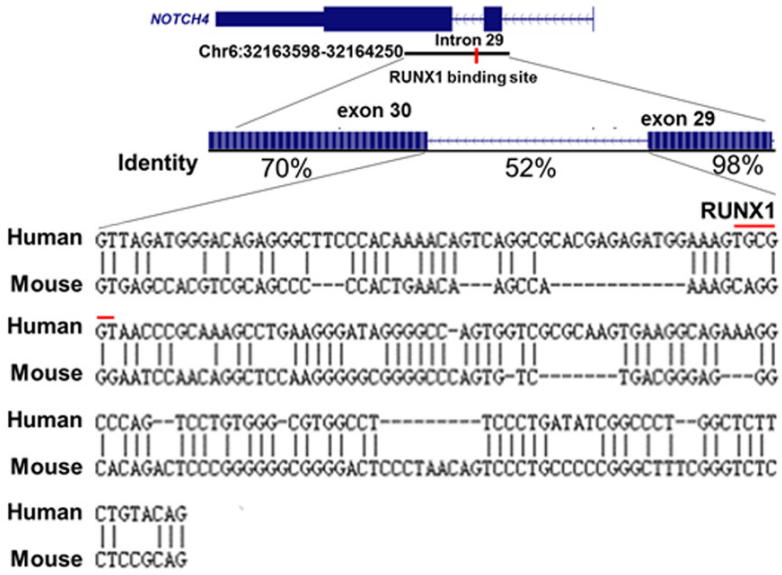

Figure S12. The RUNX1 binding site is not present in the mouse *Notch4* intron 29. The 3' region of the human *NOTCH4* gene is enlarged. The genomic location of the RUNX1 binding region determined by ChIP-Seq is marked in the gene structure as a horizontal black line and the RUNX1 consensus binding site as a vertical red line. The identity of RUNX1 binding region between human and mouse is shown. Global alignment of human and mouse *NOTCH4* intron 29 sequences with BLAST, the RUNX1 binding site in human *NOTCH4* intron 29 is marked as a horizontal red line.

Figure S13

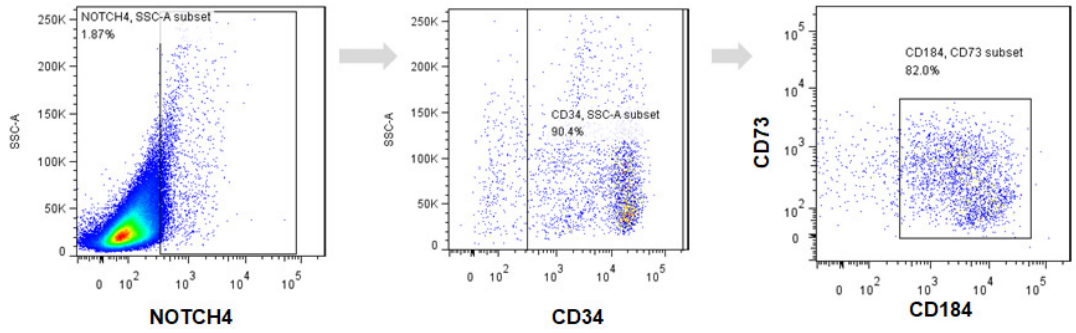

Figure S13. NOTCH4 is mainly restricted in a subpopulation of vascular endothelium (VE) ($CD34^{+}CD73^{\pm}CD184^{+}$). Representative FACS analysis of the cell population that expressed NOTCH4 at day 5 during MK differentiation from BC1 iPSCs.

Figure S14

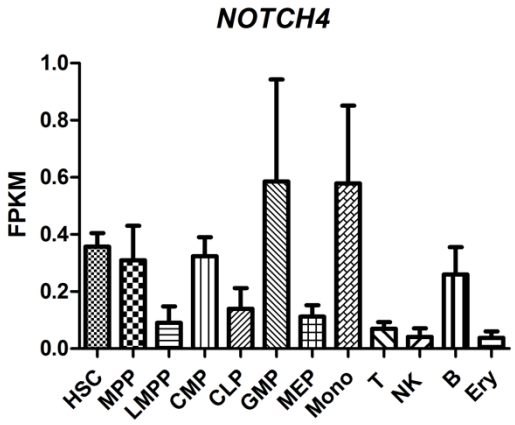

Figure S14. ***NOTCH4*** **mRNA expression is detected in HSC, and multiple progenitor cell populations from human bone marrow.** FPKM plot depicting the expression of *NOTCH4* in HSC, multiple progenitor cell populations (MPP, LMPP, CMP, CLP, GMP and MEP), and mature blood cells (mono, T, NK, B and Ery), purified from human bone marrow, by analyzing the published RNA-Seq data (GSE74246).[4] HSC, hematopoietic stem cell; MPP, multipotent progenitor; LMPP, lymphoid-primed multipotent progenitor; CMP, common myeloid progenitor; CLP, common lymphoid progenitor; GMP, granulocyte-macrophage progenitor; MEP, megakaryocyte-erythrocyte progenitor; mono, monocyte; T, T cell; NK, natural killer cell; B, B cell; Ery, erythroid.

Figure S15

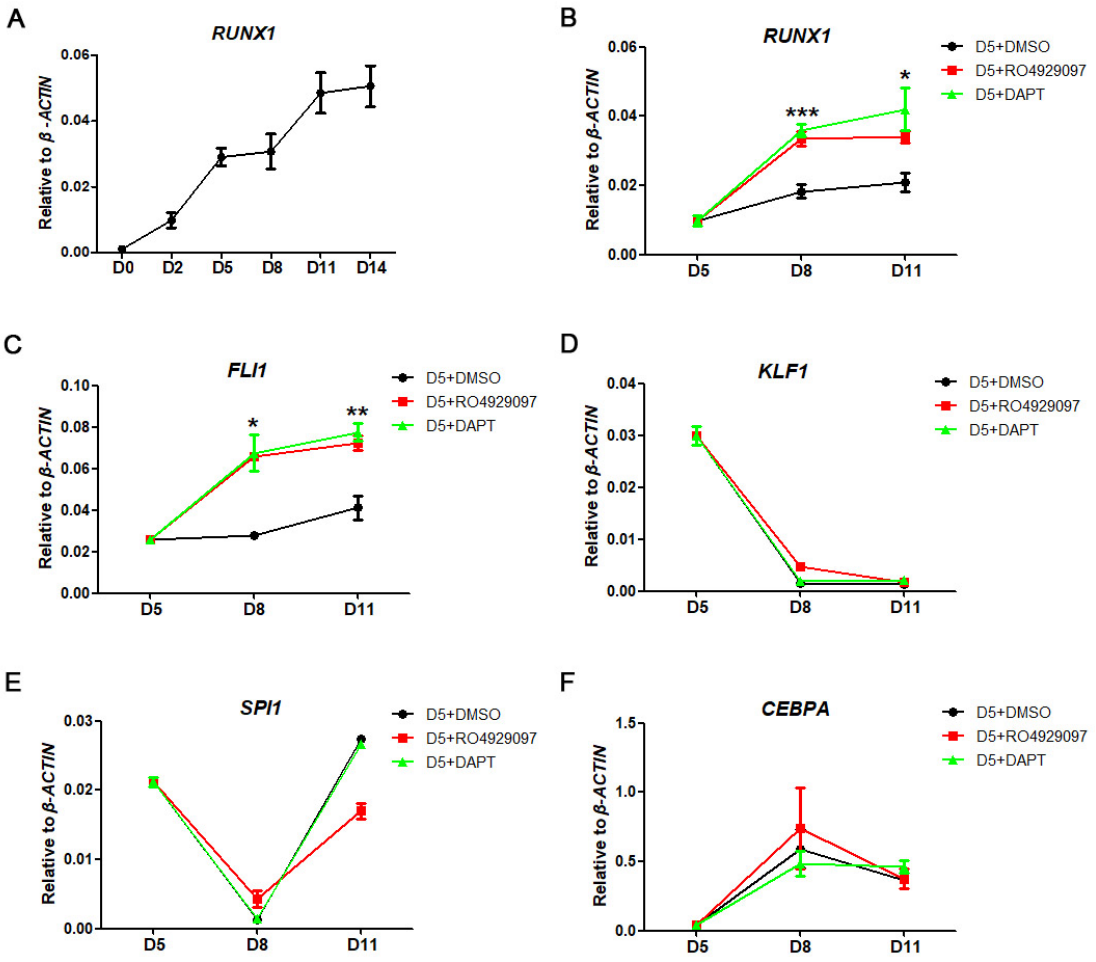

Figure S15. **GSIs increase the expression of megakaryocyte lineage specific transcription factors.** (A) RT-qPCR analysis of mRNA level of *RUNX1* at day 0, 2, 5, 8, 11 and 14 during differentiation from BC1 iPSCs. *β -ACTIN* was used as an internal control. Data are shown as means ± SEM, n = 7. (B-F) RT-qPCR analysis of mRNA level of *RUNX1* (B), *FLI1* (C), *KLF1* (D), *SPI1* (E) and *CEBPA* (F) at day 5, 8 and 11 after 10μM GSIs (RO4929097/DAPT) or DMSO (control) addition from day 5. *β -ACTIN* was used as an internal control. Data are shown as means ± SEM, n = 3. **P* < .05; ***P* < .01; ****P* < .001.

Figure S16

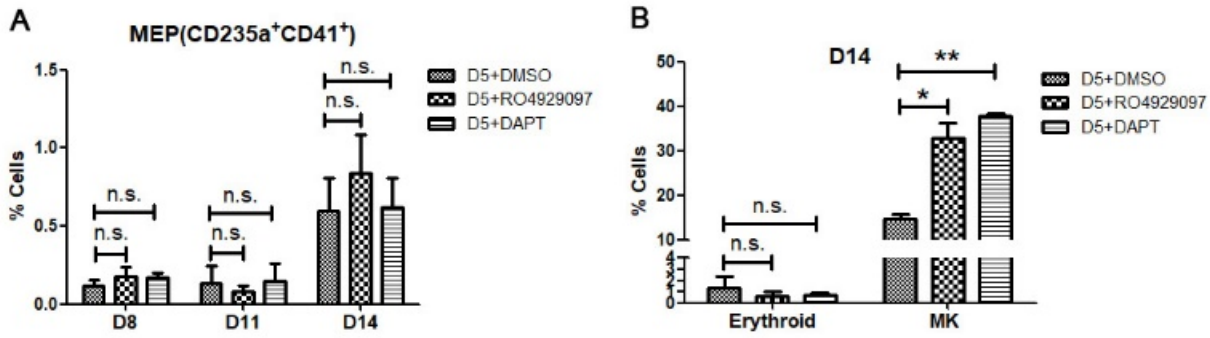

Figure S16. **The low efficiency of MEPs and erythroid cells production detected at different time points.** (A) Bar graph depicting the percentage of MEP ($CD235a^+CD41^+$) at day 8, 11 and 14 in hematopoietic cells differentiated from BC1 iPSCs, with addition of 10μM GSIs (RO4929097/DAPT) or DMSO (control) from day 5. Data are shown as means ± SEM, n = 3. n.s., no significant. (B) Bar graph depicting the percentages of erythroid cells ($CD235a^+CD41^-$) and megakaryocytes ($CD235a^-CD41^+$) on day 14 in hematopoietic cells differentiated from BC1 iPSCs, with addition of 10μM GSIs (RO4929097/DAPT) or DMSO (control) from day 5. Data are shown as means ± SEM, n = 3. *P < .05; **P < .01; n.s., no significant.

References

1. Zhou J, Wu J, Li B, et al. PU. 1 is essential for MLL leukemia partially via crosstalk with the MEIS/HOX pathway. *Leukemia*. 2014;28(7):1436-1448.
2. Tijssen MR, Cvejic A, Joshi A, et al. Genome-wide analysis of simultaneous GATA1/2, RUNX1, FLI1, and SCL binding in megakaryocytes identifies hematopoietic regulators. *Dev Cell*. 2011;20(5):597-609.
3. Consortium EP. An integrated encyclopedia of DNA elements in the human genome. *Nature*. 2012;489(7414):57-74.
4. Corces MR, Buenrostro JD, Wu B, et al. Lineage-specific and single-cell chromatin accessibility charts human hematopoiesis and leukemia evolution. *Nat Genet*. 2016;48(10):1193-1203.